Novel Soliton States and Bifurcation Phenomena in Nonlinear Fiber Couplers

Nail Akhmediev and Adrian Ankiewicz
Optical Sciences Center, Institute of Advanced Studies, Australian National University, Canberra, Australian Capital Territory 2601, Australia
(Received 4 February 1993)

We find and analyze analytically and numerically two new families of coupled soliton states in nonlinear fiber couplers. The bifurcation diagram for the new types of soliton states is constructed. It is shown that the bifurcation diagram for the fiber coupler is similar to the bifurcation diagram for the stationary waves in a symmetric nonlinear planar waveguide. Physical reasons for this analogy are discussed.

PACS numbers: 42.65.Pc, 42.81.Qb

The study of nonlinear effects in optical couplers has expanded greatly since the pioneering works of Maier [1] and Jensen [2]. One of their possible applications is to all-optical switching [3,4] and logic functions [5]. Recent experiments [6] show that very high switching speeds, e.g., in the femtosecond range, are possible with this kind of device. Extensive theoretical and numerical investigation of soliton switching and propagation dynamics has been reported in a number of publications [7–11]. In all published works, it has been implicitly or explicitly supposed that soliton states consist of two solitons having sech-function shapes. This shape is usually assumed in variational approaches in order to describe propagation [8] or other phenomena. This shape has also been used for initial conditions in numerical simulations [3,4]. In reality the shape of each component in a coupled soliton state can be quite different from the sech function. This is particularly important in considering bifurcation phenomena.

Mathematically, propagation of solitons in nonlinear fiber couplers is described by the set of two coupled nonlinear Schrödinger equations (NLSE's) with linear (and in general with nonlinear) coupling terms. In the case where only nonlinear coupling terms are present, the bifurcation of composite (vector) soliton states from one-component (polarized) soliton states has been found in [12]. These bifurcations have been studied in detail in [13]. Recently an attempt to study the same type of bifurcation (called "trivial-nontrivial") has been made in the case where only linear coupling terms are present [14]. A variational approach with trial sech functions has been used by the authors of [14]. However, this approach gives erroneous results for the envelopes of each component of the composite soliton states, for the critical bifurcation parameter, and for the bifurcation diagram in general. In this work we find two novel asymmetric soliton state families which exist in certain ranges of a normalized soliton parameter, and which can have quite complicated component envelopes. These new soliton states split off from the symmetric and antisymmetric soliton states at two different values of the soliton parameter. We construct the full bifurcation diagram for the symmetric, antisymmetric, and asymmetric soliton states, and show that there is a close analogy between the bifurcations in the nonlinear fiber coupler and those in the symmetric planar waveguide structure [15].

The propagation of pulses in a nonlinear dual-core directional coupler can be described in terms of two linearly coupled NLSE's [3]. In soliton units, this set of coupled NLSE's is given by

$$\begin{aligned} i\frac{\partial U}{\partial \xi}+\frac{1}{2}\frac{\partial^2 U}{\partial \tau^2}+|U|^2U+KV=0\,,\\ i\frac{\partial V}{\partial \xi}+\frac{1}{2}\frac{\partial^2 V}{\partial \tau^2}+|V|^2V+KU=0\,, \end{aligned} \tag{1}$$

where $U(\xi,\tau)$ and $V(\xi,\tau)$ are envelope functions and K, which is the normalized coupling coefficient between the two cores, is equal to the linear coupling coefficient times the dispersion length.

Stationary pulselike solutions (i.e., those where $d|U|/d\xi=d|V|/d\xi=0$) can be represented in the form

$$U(\xi,\tau)=u(\tau,q)e^{iq\xi},\quad V(\xi,\tau)=v(\tau,q)e^{iq\xi}, \tag{2}$$

where q is the parameter of a soliton state family of solutions and $u(\xi,q)$ and $v(\xi,q)$ are real functions decreasing to zero at infinity. Using Eq. (2), the coupled partial differential equations (1) can be reduced to the following coupled set of two real ordinary differential equations:

$$\begin{aligned} \frac{1}{2}\frac{d^2u}{d\tau^2}-qu+u^3+Kv=0\,,\\ \frac{1}{2}\frac{d^2v}{d\tau^2}-qv+v^3+Ku=0\,. \end{aligned} \tag{3}$$

By rescaling the functions and variables in (3) in such a way that

$$u=\sqrt{q}f,\quad v=\sqrt{q}g,\quad \tau=t/\sqrt{q},\quad K=q\kappa, \tag{4}$$

we transform the set (3) into the set

$$\begin{aligned} \frac{1}{2}\frac{d^2f}{dt^2}-f+f^3+\kappa g=0\,,\\ \frac{1}{2}\frac{d^2g}{dt^2}-g+g^3+\kappa f=0\,, \end{aligned} \tag{5}$$

which now has only one combined (material- and pulse-dependent) parameter κ ($=K/q$). If the initial value of K is fixed, then this combined parameter is the parameter of the soliton state family of solutions.

It is clear here from the form of Eqs. (5) that symmetric and antisymmetric soliton states are possible. The former are given by $f=g=\sqrt{2(1-\kappa)}\,\mathrm{sech}[\sqrt{2(1-\kappa)}\,t]$, where $0<\kappa<1$, while the latter are given by $f=-g=\sqrt{2(1+\kappa)}\,\mathrm{sech}[\sqrt{2(1+\kappa)}\,t]$. Applying the scaling [Eq. (4)] shows that $U=V=\sqrt{2(q-K)}\,\mathrm{sech}[\sqrt{2(q-K)}\,\tau]e^{iq\xi}$ are the symmetric solutions of (1),(2) for any $q>K$, while $U=-V=\sqrt{2(q+K)}\,\mathrm{sech}[\sqrt{2(q+K)}\,\tau]e^{iq\xi}$ are the antisymmetric solutions for all $q>0$. This form of the soliton states shows that it is more convenient to change variables to

$$f=(x+y)/\sqrt{2},\quad g=(x-y)/\sqrt{2}. \tag{6}$$

In this case Eqs. (5) can be written in the form

$$\ddot{x}-\alpha^2x+x^3+3xy^2=0, \tag{7a}$$

$$\ddot{y}-\mu^2\alpha^2y+y^3+3yx^2=0, \tag{7b}$$

where $\alpha^2=2(1-\kappa)$, $\mu=[(1+\kappa)/(1-\kappa)]^{1/2}$, and each dot means derivative with respect to t. If $\kappa>1$ then the second term in (7a) changes sign and the symmetric soliton state does not exist. Antisymmetric soliton states exist for any positive κ.

Equations (7) can be considered as governing the motion of a particle in a two-dimensional potential well. The Hamiltonian for this motion is

$$H=\tfrac{1}{2}\dot{x}^2+\tfrac{1}{2}\dot{y}^2-(x^2+y^2)+\kappa(x^2-y^2)+\tfrac{1}{2}(x^2+y^2)^2-\tfrac{1}{4}(x^2-y^2)^2. \tag{8}$$

Comprehensive analysis of this type of Hamiltonian with arbitrary coefficients in front of the nonlinear terms in (8) was done in [16]. This analysis shows that only special cases are integrable. Our Hamiltonian (8) belongs to the nonintegrable class. We will analyze soliton states of (7) and their bifurcations using methods like those in [12] and [13].

Solitons are the solutions of the set (7) with $H=0$ (as we require $\dot{x},\dot{y}\to 0$ when $x,y\to\infty$). This means that all trajectories corresponding to soliton states must be contained within the curve

$$(x^2+y^2)-\kappa(x^2-y^2)-\tfrac{1}{4}(x^4+y^4)-\tfrac{3}{2}x^2y^2=0, \tag{9}$$

or, in polar coordinates ($x=r\cos\varphi$, $y=r\sin\varphi$),

$$r^2=4(1-\kappa\cos2\varphi)/(1+\sin^2 2\varphi). \tag{10}$$

Each component of the composite soliton states we are studying here is a symmetric function in t for both x and y. This means that $\dot{x},\dot{y}=0$ at the soliton center. Hence, the center of symmetry points (which we define as $t=0$) of the soliton states are located on the curve given by Eqs. (9),(10). We define this point as (x_0,y_0), and the corresponding angle with the x axis, φ, as the coupling angle $\varphi_0=\arctan(y_0/x_0)$.

The set of equations (7) has simple soliton states at $\varphi_0=0$,

$$x(t,\kappa)=\sqrt{2}\,\alpha\,\mathrm{sech}(\alpha t),\quad y=0, \tag{11}$$

and at $\varphi_0=90°$,

$$x=0,\quad y(t,\kappa)=\sqrt{2}\,\alpha\mu\,\mathrm{sech}(\alpha\mu t), \tag{12}$$

which correspond to symmetric and antisymmetric states in the initial variables f and g, respectively. We recall that solution (11) exists for $0<\kappa<1$, while solution (12) exists for any $\kappa>0$.

In order to study the bifurcation from the state (11), we represent the solution of Eqs. (7) as a soliton (11) with an added small perturbation:

$$x=\sqrt{2}\,\alpha\,\mathrm{sech}(\alpha t)+\varepsilon^2F, \tag{13a}$$

$$y=\varepsilon G, \tag{13b}$$

where ε is a small parameter. The linear term in ε in (13a) is zero. Substituting (13) into (7), and linearizing with respect to the small parameter ε, we find

$$G_{tt}-\mu^2\alpha^2G+(6\alpha^2/\cosh^2\alpha t)G=0. \tag{14}$$

Equation (14) has exactly two solutions which decay at infinity. They are an odd solution,

$$G=\sinh\alpha t/\cosh^2\alpha t\quad(\text{at }\mu=1), \tag{15}$$

and an even solution,

$$G=\mathrm{sech}^2\alpha t\quad(\text{at }\mu=2). \tag{16}$$

The odd solution (15) does not correspond to any bifurcation because $\kappa=0$ at $\mu=1$ and x and y become decoupled in this limit. The even solution (16) makes the symmetric soliton state asymmetric at the point $\mu=2$ (i.e., $\kappa=0.6$). Hence $\kappa=0.6$ is the point of bifurcation of these asymmetric soliton states from the symmetric ones. We shall call these states "A-type" asymmetric states. We can see from this simple analysis that these new states cannot be represented as sech functions. Even to the lowest order, these states are combinations of two different functions. The consequence is that, at high $|t|$, A-type states depend on two exponentials, while the simple sech function depends on only one.

A separate asymmetric soliton state bifurcates from the antisymmetric states at $\kappa=1$. We shall call these states "B-type" asymmetric soliton states. This is a more complicated type of bifurcation, and it cannot be analyzed using perturbative analysis. The reason is that at $\kappa\to 1$, the value α in (7a) goes to zero. This means that the decrease of x at $t\to\pm\infty$ can be much slower than the decrease of y. In other words the condition $x\ll y$ cannot be fulfilled for all t simultaneously and we have to study the set (7) for all κ in general, and close to this particular point, using numerical methods.

In general, i.e., not only close to the points of bifurcation, in these asymmetric soliton states, both variables x and y are nonzero. They are located on the curve $y=y(x)$ in the plane (x,y). It can be shown using (7) and the condition $H=0$ that this curve is defined by the following differential equation:

$$y_{xx}[\alpha^2x^2+\alpha^2\mu^2y^2-\tfrac{1}{2}(x^4+y^4)-3x^2y^2]+(1+y_x^2)[y_x(\alpha^2x-x^3-3xy^2)+y^3-\alpha^2\mu^2y+3yx^2]=0. \quad (17)$$

The approximate solution at small x is $y=Ax^{\mu}$ with $A=A(\kappa)$. The intersection of this curve with the curve (10) defines the point (x_0,y_0) and the coupling angle φ_0. Examples of these curves, calculated numerically, for A- and B-type soliton states, are given in Fig. 1.

A-type soliton states exist in a range $0<\kappa<0.6$, while the B-type soliton states exist in the range $0<\kappa<1$. The bifurcation diagram for these two types of soliton states is shown in Fig. 2. At the left end of these two intervals ($\kappa=0$), the soliton states degenerate into decoupled solitons. Note that, in this limit, the B-type soliton state transforms into three decoupled solitons. This transition is clearly seen in Fig. 1(b). The distance between these three solitons goes to infinity when κ goes to zero. On the other hand, the A-type soliton state degenerates into a single soliton. On the right of each interval, the solitons degenerate into simple symmetric and antisymmetric soliton states at bifurcation points M and N, respectively. As a result of the symmetry of Eqs. (7) relative to the change of signature of each of the functions x and y, the bifurcation diagram in Fig. 2 can be extended to φ_0 values less than zero and more than 90° by taking mirror images of the given one.

Numerical examples of B-type asymmetric soliton states are given in Fig. 3. When $\kappa=0.5$, each component of the soliton state has a complicated shape which is completely different from the simple sech function at $\kappa=1$. Decreasing the κ value causes splitting of the vector soliton into three independent solitons as seen in Fig. 3(b). Two of them are polarized along the g axis while the third is polarized along the f axis. The distance between separate solitons gradually increases with decreasing κ.

The total energy carried by the coupled soliton states is defined by

$$Q=\int_{-\infty}^{\infty}(|U|^2+|V|^2)d\tau=\sqrt{q}\int_{-\infty}^{\infty}(x^2+y^2)dt. \quad (18)$$

The curves $Q(q)$, with Q and q normalized by coupling constant K, for the four different types of soliton states, are shown in Fig. 4. This bifurcation diagram is similar to the diagram for the waves in the symmetric nonlinear waveguide found in [15]. Two new branches of asymmetric solutions (corresponding to type-A and type-B soliton states) split off from the dispersion curves for symmetric and antisymmetric solutions at bifurcation points M and N, respectively. The total energies Q of symmetric and antisymmetric solutions have the same limit at $q\to\infty$ (i.e., $\kappa\to 0$). This is not unusual because the physical phenomena in these two cases are also quite similar. The waveguide structure considered in [15] consists of two nonlinear media with a linear layer between

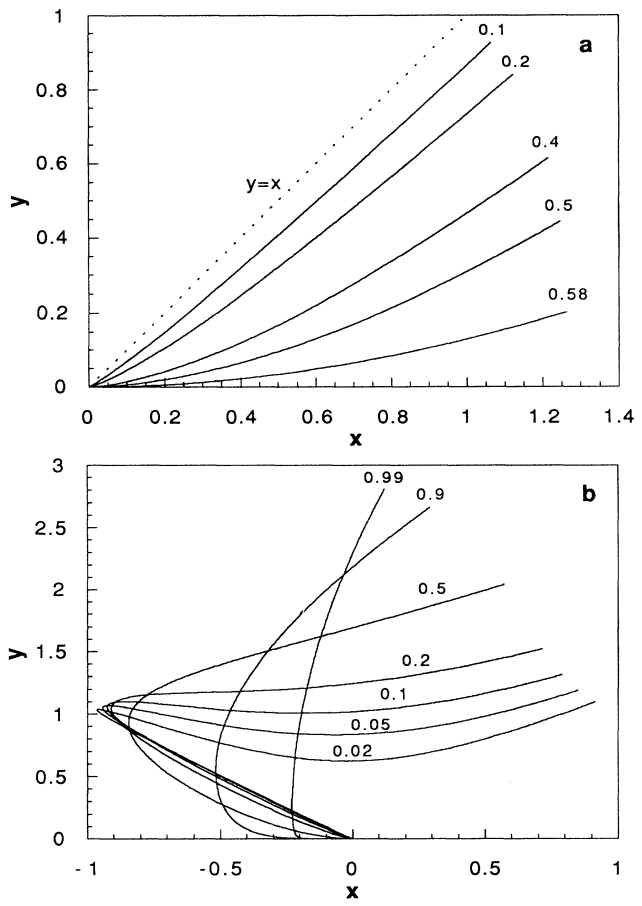

FIG. 1. Parametric curves for type-A (a) and type-B (b) soliton states in the (x,y) plane. The curves are labeled with the value of combined parameter κ. The variable t is the parameter for these curves. The point (0,0) corresponds to $t=\pm\infty$ while $t=0$ corresponds to the other end of each curve [i.e., (x_0,y_0)].

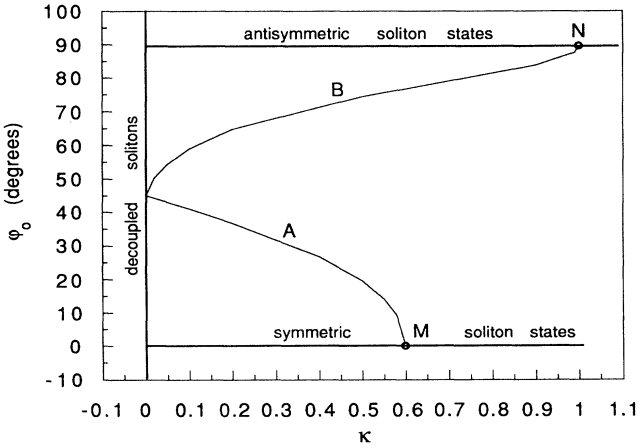

FIG. 2. Bifurcation diagram on (φ_0,κ) plane. Solid curves correspond to different types of soliton states. Circles M and N are the points of bifurcation.

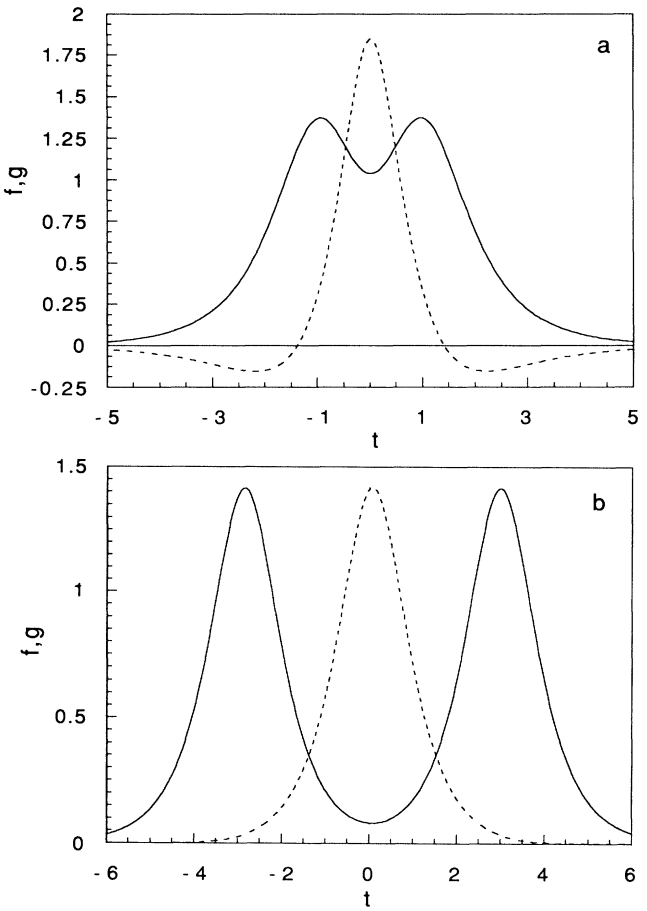

FIG. 3. Examples of the B-type soliton states for (a) $\kappa=0.5$ and (b) $\kappa=0.01$. Solid curves represent the function $-g$, and dashed curves represent the function f of the composite asymmetric soliton state.

them. This structure can be considered as two self-focusing nonlinear waveguides, coupled linearly through the central layer [17]. Although the two situations are similar, they are not completely identical. In particular, the linear interaction between the field components in this case is distributed along the t variable, in contrast to the case considered in [15] where the interaction is concentrated on the interfaces. One of the consequences is that the B-type soliton state consists of three decoupled solitons in the limit $q \to \infty$. Correspondingly, Q values for B-type states are 3 times larger than Q values for A-type states in this limit. On the other hand, this close analogy shows that the stability of new soliton states can be considered using methods developed for the symmetric nonlinear waveguide problems [17].

In conclusion, we have found two new families of composite soliton states in nonlinear directional couplers and constructed the bifurcation diagram for them. We have shown that a close similarity exists between the bifurcation diagram for this problem and that for the waves in a symmetric nonlinear waveguide with linear core.

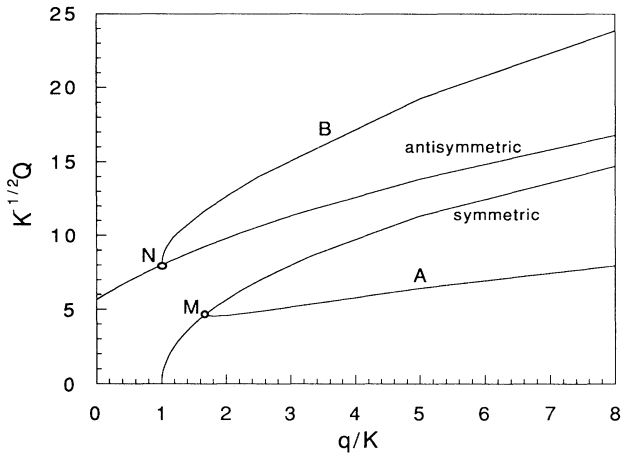

FIG. 4. Bifurcation diagram on (Q,q) plane, where Q is the total state energy given by Eq. (18). Both variables are normalized. Labeling is the same as in Fig. 2.

The authors acknowledge fruitful discussions with Dr. G. D. Peng.

[1] A. M. Maier, Kvantovaya Elektron. (Moscow) **9**, 2296 (1982) [Sov. J. Quantum Electron. **12**, 1490 (1982)].
[2] S. M. Jensen, IEEE J. Quantum Electron. **18**, 1580 (1982).
[3] S. Trillo, S. Wabnitz, E. M. Wright, and G. I. Stegeman, Opt. Lett. **13**, 672 (1988).
[4] J. Wilson, G. I. Stegeman, and E. M. Wright, Opt. Lett. **16**, 1653 (1991).
[5] C. C. Yang, Opt. Lett. **16**, 1641 (1991).
[6] S. F. Friberg, A. M. Weiner, Y. Silberberg, B. G. Sfez, and P. S. Smith, Opt. Lett. **13**, 904 (1988).
[7] G. D. Peng and A. Ankiewicz, Int. J. Nonlinear Opt. Phys. **1**, 135 (1992).
[8] Y. S. Kivshar, Opt. Lett. **18**, 7 (1993).
[9] F. Kh. Abdullaev, R. M. Abrarov, and S. A. Darmanyan, Opt. Lett. **14**, 131 (1989).
[10] F. Kh. Abdullaev and A. A. Abdumalikov, Pis'ma Zh. Tekh. Fiz. **14**, 1041 (1988) [Sov. Tech. Phys. Lett. **14**, 458 (1988)].
[11] See papers in special issue on soliton switching, Opt. Quant. Electronics **24** (November 1992).
[12] N. N. Akhmediev, V. M. Eleonskii, N. E. Kulagin, and L. P. Shil'nikov, Pis'ma Zh. Tekh. Fiz. **15**, 19 (1989) [Sov. Tech. Phys. Lett. **15**, 587 (1989)].
[13] V. M. Eleonskii, V. G. Korolev, N. E. Kulagin, and L. P. Shil'nikov, Zh. Eksp. Teor. Fiz. **99**, 1113 (1991) [Sov. Phys. JETP **72**, 619 (1982)].
[14] P. L. Chu, B. A. Malomed, and G. D. Peng, in *Proceedings of the Seventeenth Australian Conference on Optical Fibre Techniques, Hobart, Australia, 1992*, edited by Peter Taylor (The Institution of Radio and Electronic Engineers Australia, Sydney, 1992), p. 266.
[15] N. N. Akhmediev, Zh. Eksp. Teor. Fiz. **83**, 545 (1982) [Sov. Phys. JETP **56**, 299 (1982)].
[16] M. Lakshmanan and R. Sahadevan, Phys. Rev. A **31**, 861 (1985).
[17] N. N. Akhmediev, A. Ankiewicz, and H. T. Tran, J. Opt. Soc. Am. B (to be published).